

Heavy Ion Test Plan for the RH6105MW

Dakai Chen, Andy Mo, and Tom Decker

Test Date: September 11th, 2018

I. Introduction

The purpose of this test was to determine the heavy ion-induced single-event effect (SEE) susceptibility of the RH6105 from Analog Devices.

II. Device Under Test

The RH6105 is a Micropower Precision, Rail-to-Rail Input Current Sense Amplifier. The device is suitable for a wide range of RF and microwave applications. The device is built on a proprietary bipolar process that is radiation hardened for total-ionizing dose irradiation (TID). Figure 1 shows the pin configuration for the device in a W-10 ceramic Flatpack. Table I shows the basic part and test details. Detailed device parameters and functional descriptions can be found in the datasheet [1].

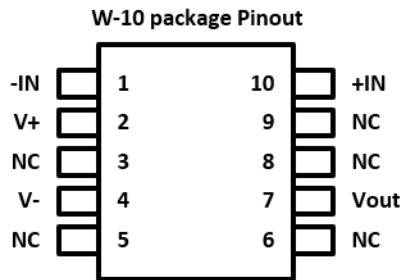


Figure 1. Schematic of the pin configuration.

Table I
Part and test information.

Part Number:	RH6105MW
Manufacturer:	Analog Devices, Inc.
Fab Lot Number:	712546.2
Quantity Tested:	2
Serial Numbers of Radiation Samples:	B, C
Part Function:	Current sense amplifier
Part Technology:	Bipolar
Package Style:	10-lead ceramic Flatpack
Test Equipment:	Agilent DSO6034A oscilloscope (SN: MY44002742) Power supply, and Laptop

III. Test Facility

The heavy-ion testing was carried out at the Lawrence Berkeley National Laboratory (LBNL) Berkeley Accelerator Space Effects (BASE) Facility utilizing an 88-inch cyclotron [2]. The irradiation was conducted in vacuum.

Facility:	LBNL
Cocktail:	10 MeV/nucl
Flux:	$\sim 10^3$ to 10^4 ions/cm ² /s
Fluence:	$\sim 10^5$ to 10^7 ions/cm ² per run
Ions:	Shown in Table II

Table II
Heavy-ion specie, linear energy transfer (LET) value, range, and energy.

Ion	LET (MeV·cm ² /mg)	Range in Si (μ m)	Energy (MeV)
Ne	3.5	175	216
Ar	9.7	130	400
Cu	21.1	108	659
Xe	58.8	90	1232

IV. Test Method

A. Test Setup

Figure 2 shows a schematic diagram of the test circuit. We evaluated two variants of the test circuit with different sense and output load resistor values. Configuration B has a gain of 500 and the following resistor values: $R_L = 49.9 \text{ k}\Omega$ and $R_{\text{Sense}} = 3.65 \text{ }\Omega$. Configuration A has a gain of 5000 and the following resistor values: $R_L = 499 \text{ k}\Omega$ and $R_{\text{Sense}} = 0.365 \text{ }\Omega$.

The source voltage was varied during the test from 3 V to 30 V. The output voltage was approximately half of the source voltage. The output was connected to an oscilloscope. A custom Python script automated the transient capture process. The appropriate trigger levels for the oscilloscope ($\sim 50 \text{ mV}$) accounted for the background noise level at the test site.

Figure 3 shows a schematic diagram of the setup at the facility. The user control room is located above the beam chamber. The device-under-test (DUT) and all necessary equipment (e.g. power supply, signal generator, oscilloscope) were located in the beam chamber. The equipment were interfaced to the user PCs using USB and extension cables routed to the control room via a cable-drop access opening across the rooms. Figure 4 shows photograph of the onsite setup.

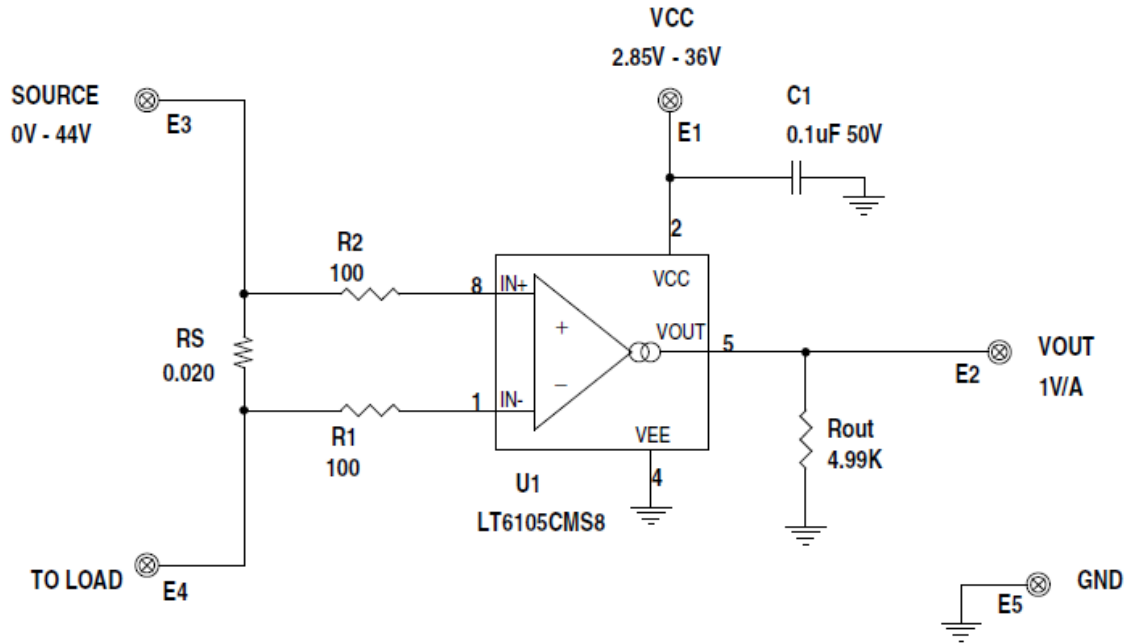


Figure 2. Schematic of the test circuit.

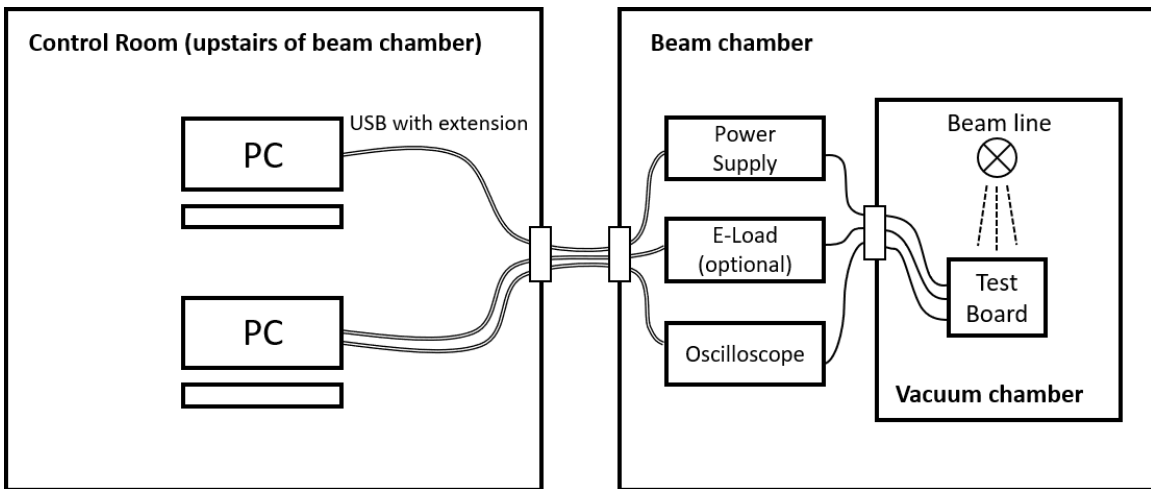


Figure 3. Schematic diagram of the test setup at LBNL.

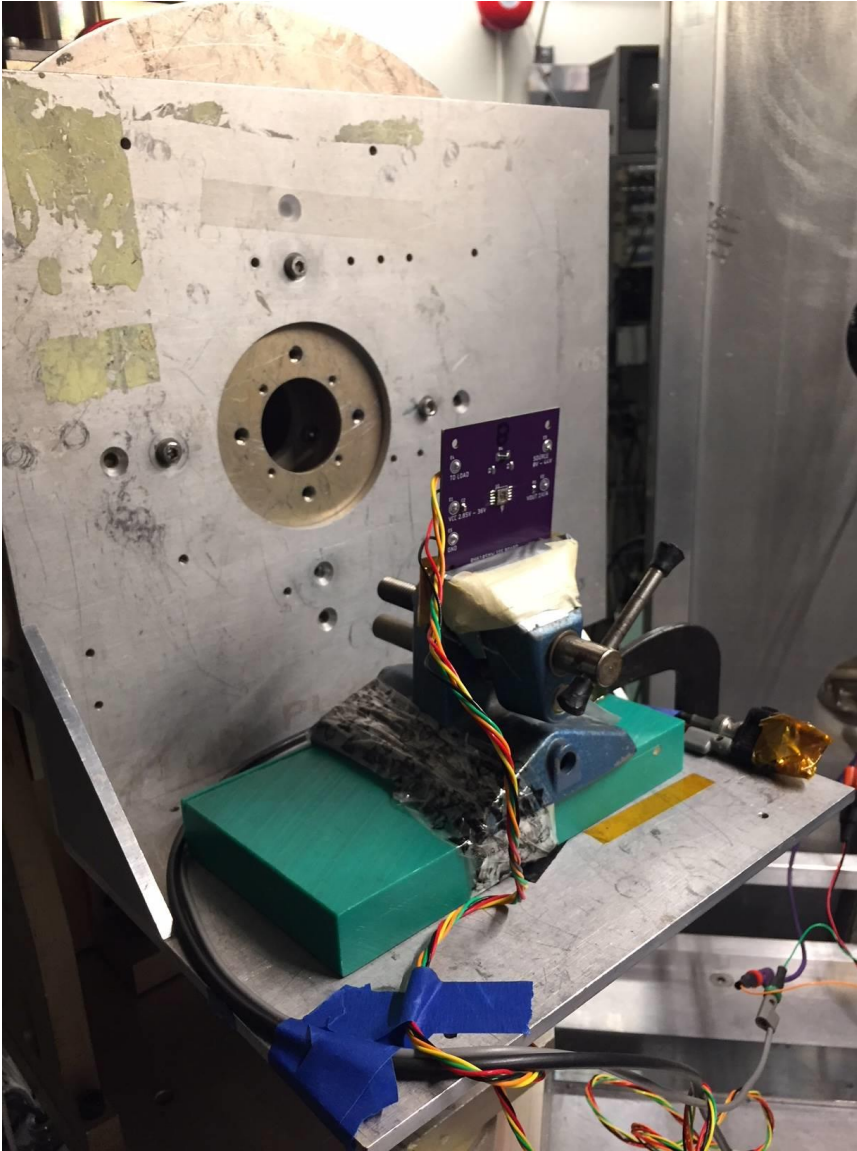


Figure 4. Photograph of the setup.

B. Irradiation procedure

The DUTs were decapsulated for the irradiation. The irradiation procedures followed JESD57A Test Procedures for the Measurement of Single-event Effects in Semiconductor Devices from Heavy Ion Irradiation [3].

C. Test Conditions

Test Temperature:	Ambient temperature
Operating Frequency:	DC
Power Supply (V_{cc}):	20 or 30 V
Source (V_s):	3, 6, 12, 20, and 30 V
Parameters to record:	1) Supply current 2) Output voltage

V. Results

We found that the RH6105MW was susceptible to single-event transients (SET). We did not observe any destructive event or high current event for the applied test conditions up to a highest effective LET of 83.2 MeV·cm²/mg. The effective fluence at an effective LET of 83.2 MeV·cm²/mg was greater than 10⁷ cm⁻². Figure 5 shows the SET cross section as a function of effective LET for positive-going transients. The negative-going SETs have approximately the same cross sections, as shown in Figure 6. The Weibull fit parameters are shown in Table III. We assumed a LET threshold of 3 MeV·cm²/mg. Only 1 SET was observed (circuit configuration C) at a LET of 3.5 MeV·cm²/mg up to a fluence of $\sim 4 \times 10^6$ cm⁻². The error bars represent Poisson error at the upper 95% confidence interval. The error bars are smaller than data symbols when not visible.

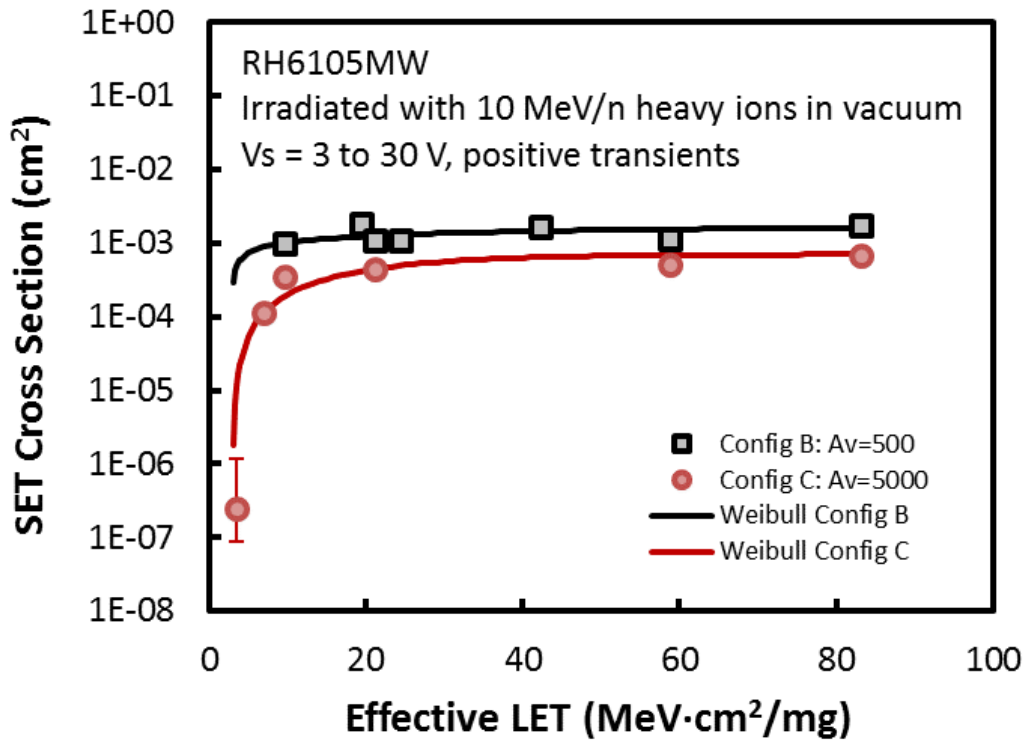


Figure 5. SET cross section vs. effective LET for the RH6105MW irradiated with 10 MeV/n heavy ions in vacuum. The SET cross section includes all transients captured using positive trigger.

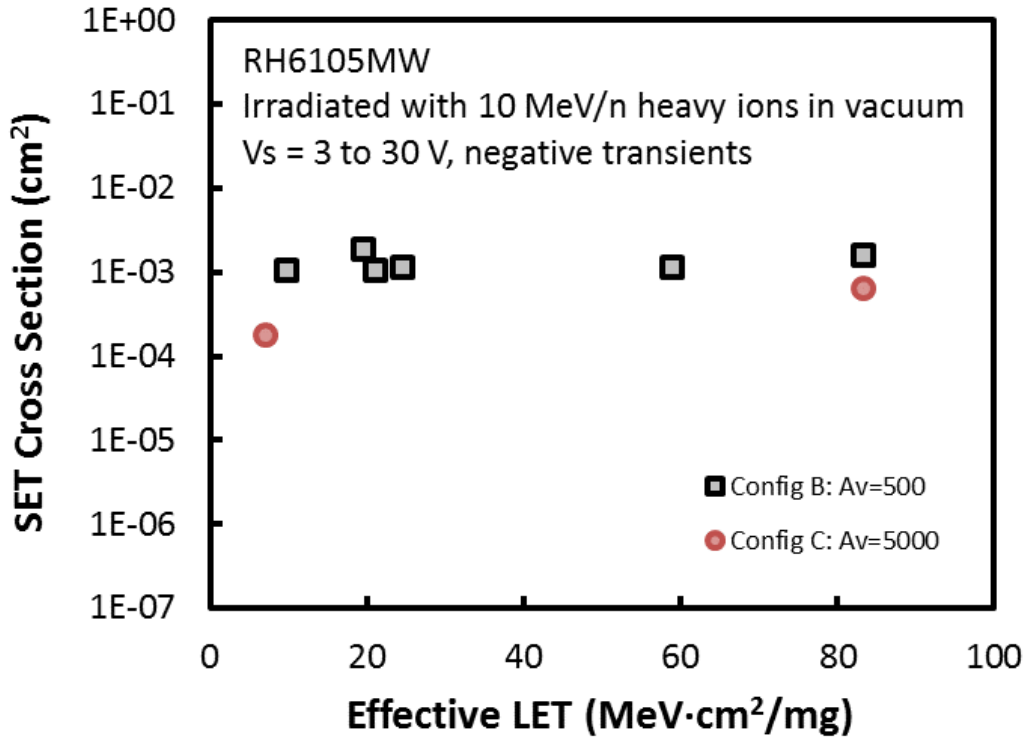


Figure 6. SET cross section vs. effective LET for the RH6105MW irradiated with 10 MeV/n heavy ions in vacuum. The SET cross section includes all transients captured using negative trigger.

Table III
Weibull parameters for SET cross sections shown in Figure 5.

Parameter	Config B (Av = 500)	Config B (Av = 5000)	Unit
LET ₀	3	3	MeV·cm ² /mg
Sigma	2 × 10 ⁻³	7 × 10 ⁻⁴	cm ²
Exponent	0.35	1.15	NA
Width	19	18	MeV·cm ² /mg

Figures 5 and 6 show that the device SET cross section curve is higher for configuration B with a gain of 500 than for configuration C with a gain of 5000. However, each configuration represented one test sample. So, one would have to be mindful of part-to-part variability in these results. Figure 7 shows the SET cross section dependence on the source voltage (V_s). There is a slight increase in SET sensitivity at 30 V relatively to the lower values, but otherwise the changes over V_s is negligible. Figure 8 shows the angular dependence of the SET cross section at an effective LET of ~ 20 MeV·cm²/mg, obtained using irradiation with Cu at normal incidence (19.5 MeV·cm²/mg) and 30° (24.4 MeV·cm²/mg), and Ar at 60° (21.1 MeV·cm²/mg). The device exhibited an enhanced SET sensitivity from 30° to 60° tilt angle. The angular

dependence is also evident in Figure 5, where we observe “spikes” in the cross section at 45° and 60° but not at 30°.

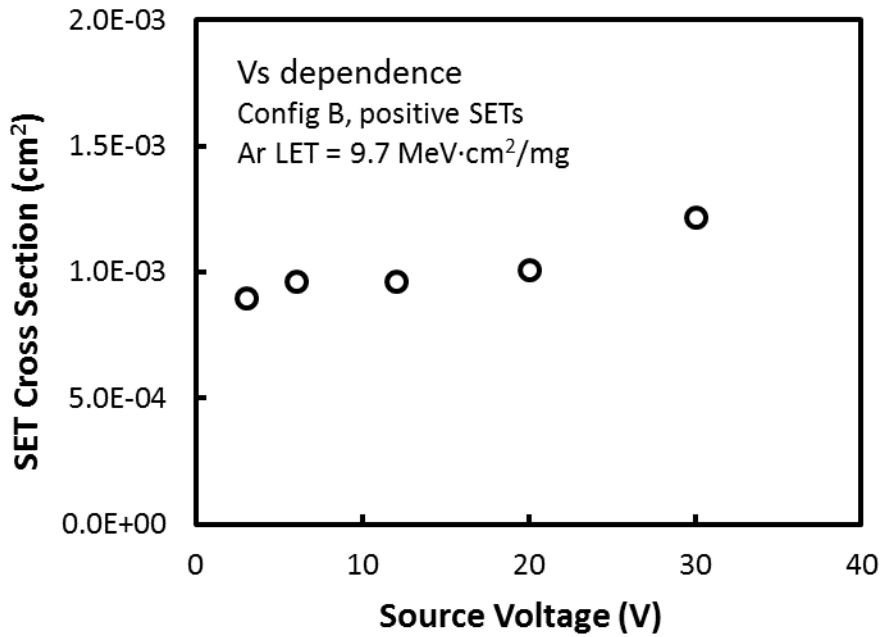


Figure 7. SET cross section vs. source voltage for the RH6105MW irradiated with 10 MeV/n heavy ions in vacuum.

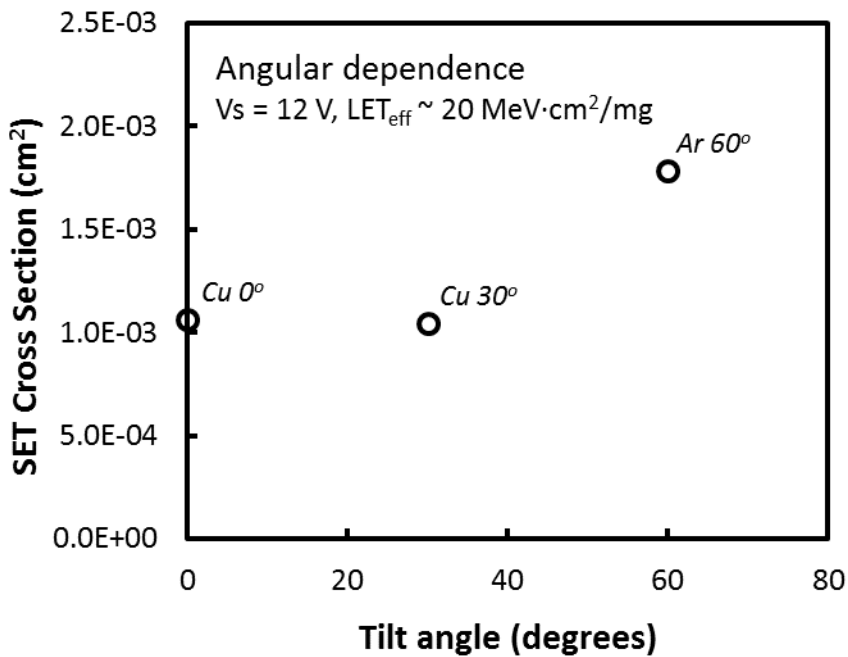


Figure 8. SET cross section vs. angle for the RH6105MW irradiated with 10 MeV/n heavy ions in vacuum. Irradiation with Cu at 0° and 30° results in LET and effective LET of 19.5 and 24.4 MeV·cm²/mg, respectively. Irradiation with Ar at 60° results in an effective LET of 21.1 MeV·cm²/mg.

Figure 9 shows a scatter plot of all SETs captured during the test, color shaded by the effective LET. The SET duration is determined by the full-width-half-maximum (FWHM) value. Notably, the SET magnitude increases with increasing LET, with more higher amplitude and longer duration SETs captured at higher effective LETs. Figure 10 shows a scatter plot of SETs grouped by the dc gain. There is a higher proportion of SETs with longer durations at a higher gain of 5000 than at the lower gain of 500. Also, there are SETs with large amplitudes of up to 8 V at a gain of 5000, whereas those SETs are missing at a gain of 500.

Figure 11 and 12 show the waveforms of all SETs captured during runs at a LET of $9.74 \text{ MeV}\cdot\text{cm}^2/\text{mg}$, for V_s of 3 V and 30 V, respective. There are proportionally more SETs with slightly higher amplitudes at 30 V than at 3 V, although the difference is not significant. Figure 13 shows the waveforms captured during a run at a LET of $58.8 \text{ MeV}\cdot\text{cm}^2/\text{mg}$, for V_s of 30 V. The SETs at the higher LET are significantly larger in amplitude, although not necessarily longer in duration, than those at the lower LET shown in Figure 12. Some of the larger amplitudes are clipped by the power supply limits. Figure 13 shows the SETs captured for a run at LET of $9.74 \text{ MeV}\cdot\text{cm}^2/\text{mg}$, for V_s of 30 V in Configuration C ($A_v = 5000$). The SET durations for the high gain configuration are longer relative to those at a lower gain configuration, as shown in Figure 12. Also, the SET amplitudes are slightly larger at a higher dc gain, although to a lesser extent than the magnitude of the increase in the SET widths. These characteristics are consistent with the amplitude vs. width distributions illustrated in Figure 10. Figures 15 to 17 show examples of SETs.

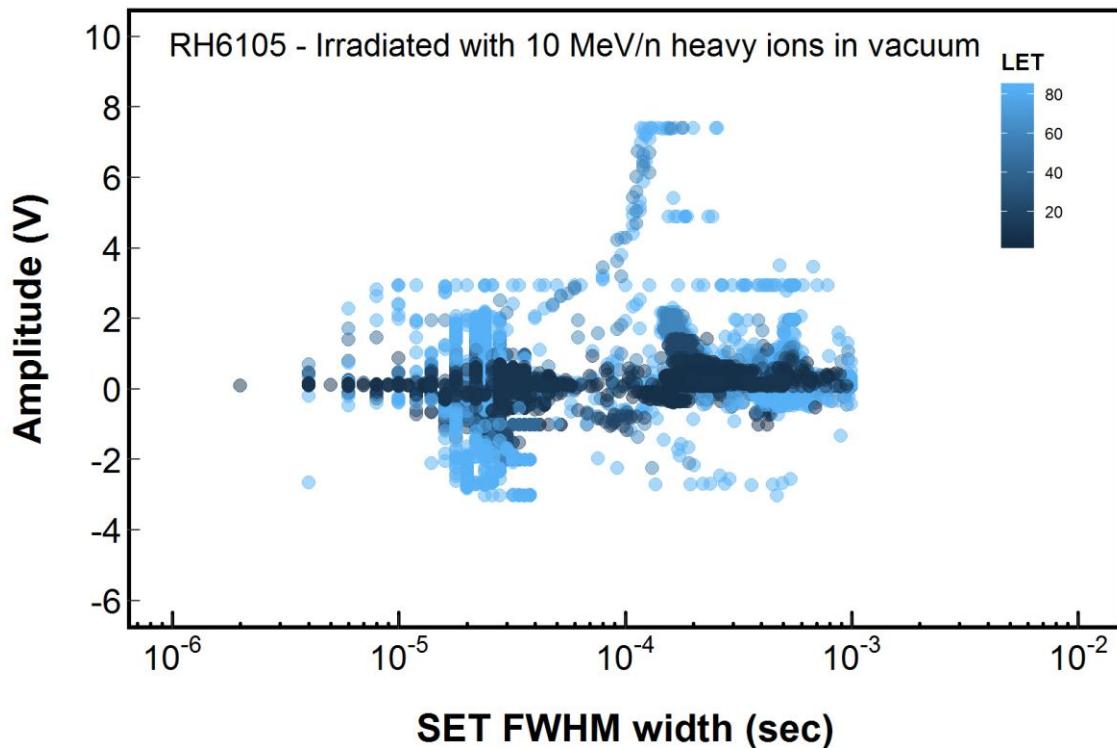


Figure 9. Scatterplot of SET amplitude and width grouped by the effective LET value, for the RH6105MW irradiated with 10 MeV/n heavy ions in vacuum.

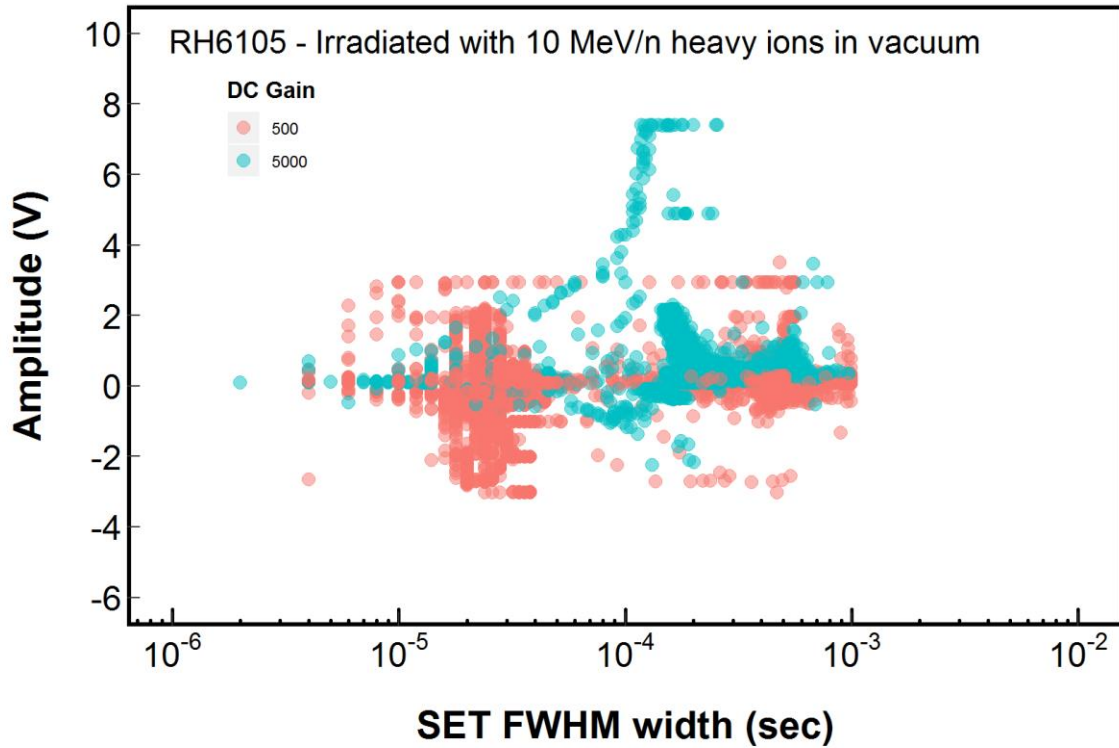


Figure 10. Scatterplot of SET amplitude and width grouped by the circuit dc gain, for the RH6105MW irradiated with 10 MeV/n heavy ions in vacuum.

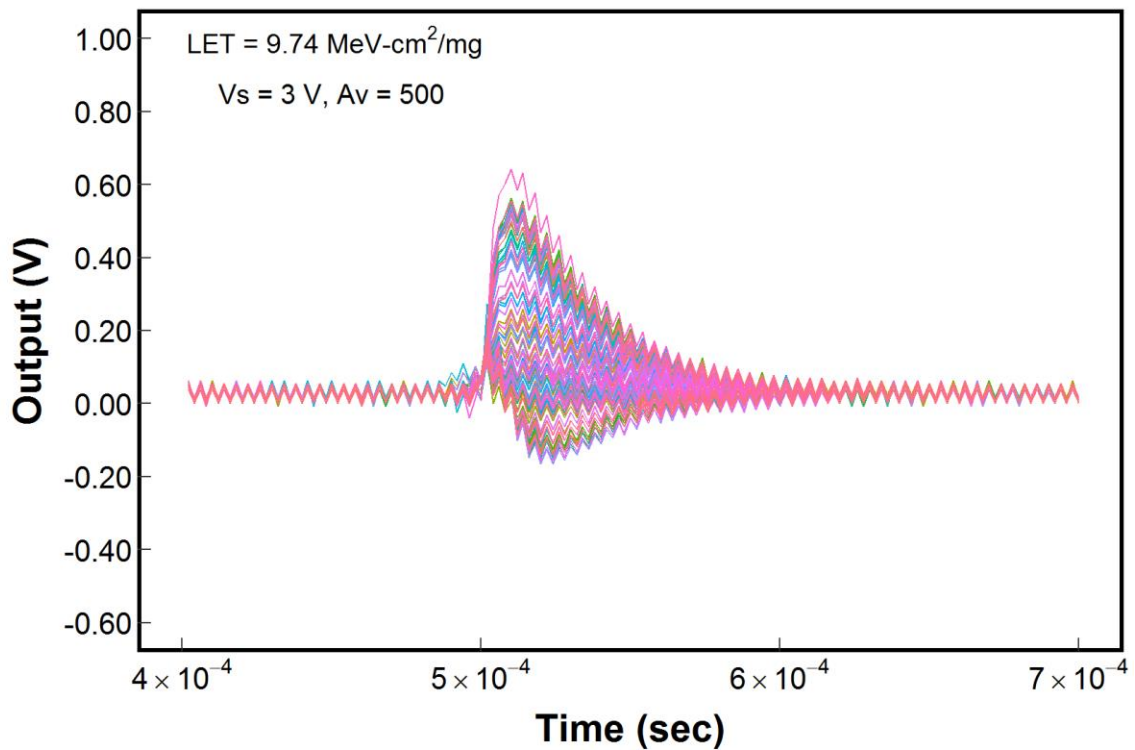


Figure 11. Output amplitude vs. time for SETs captured at LET of 9.74 MeV·cm²/mg for V_s = 3 V.

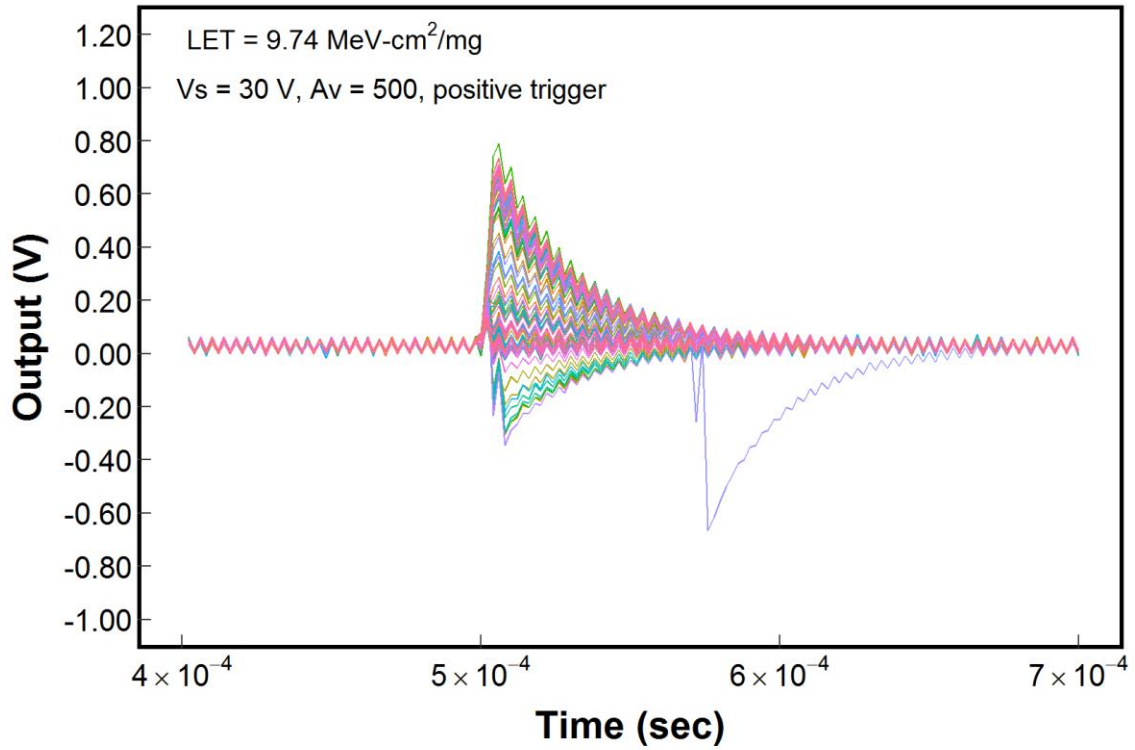


Figure 12. Output amplitude vs. time for SETs captured at LET of 9.74 MeV·cm²/mg for V_s = 30 V.

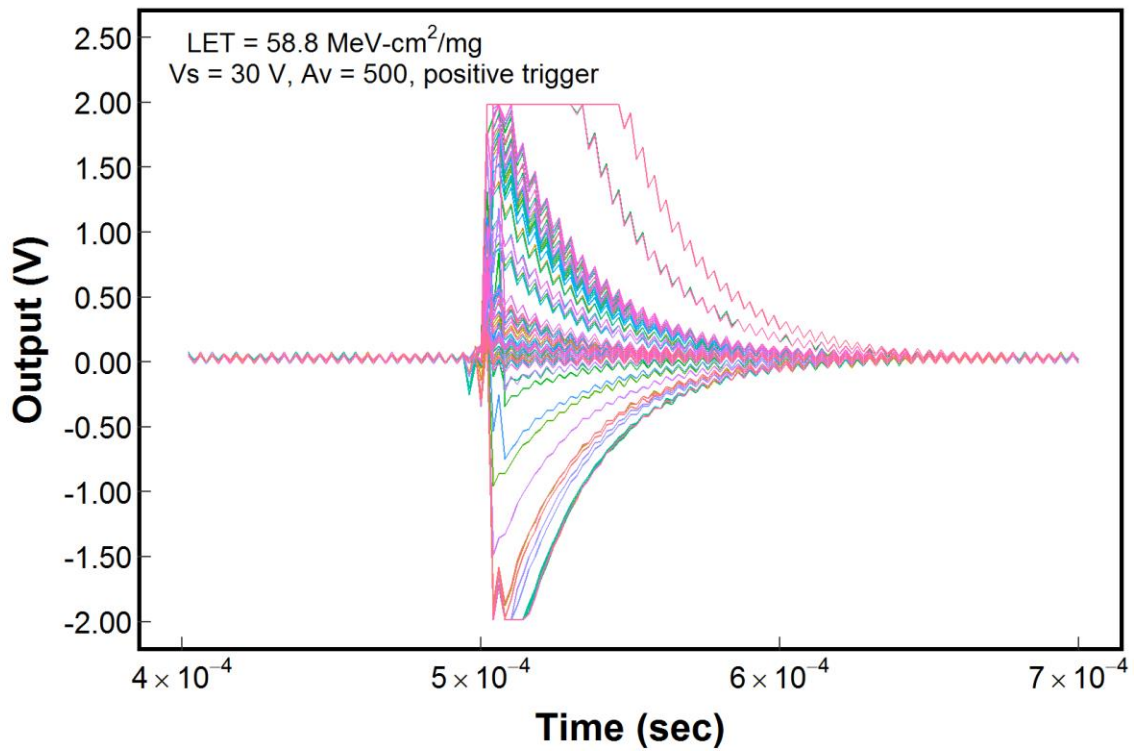


Figure 13. Output amplitude vs. time for SETs captured at LET of 58.8 MeV·cm²/mg for V_s = 30 V.

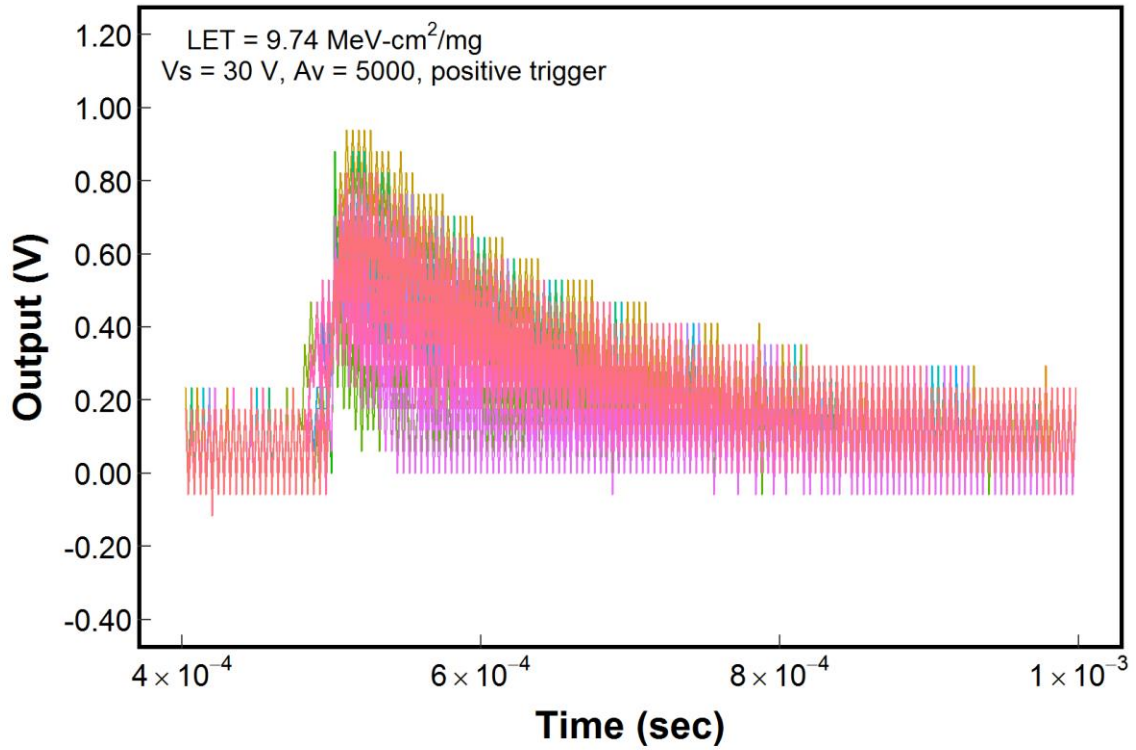


Figure 14. Output amplitude vs. time for SETs captured at LET of $9.74 \text{ MeV}\cdot\text{cm}^2/\text{mg}$ for $V_s = 30 \text{ V}$ and $A_v = 5000$.

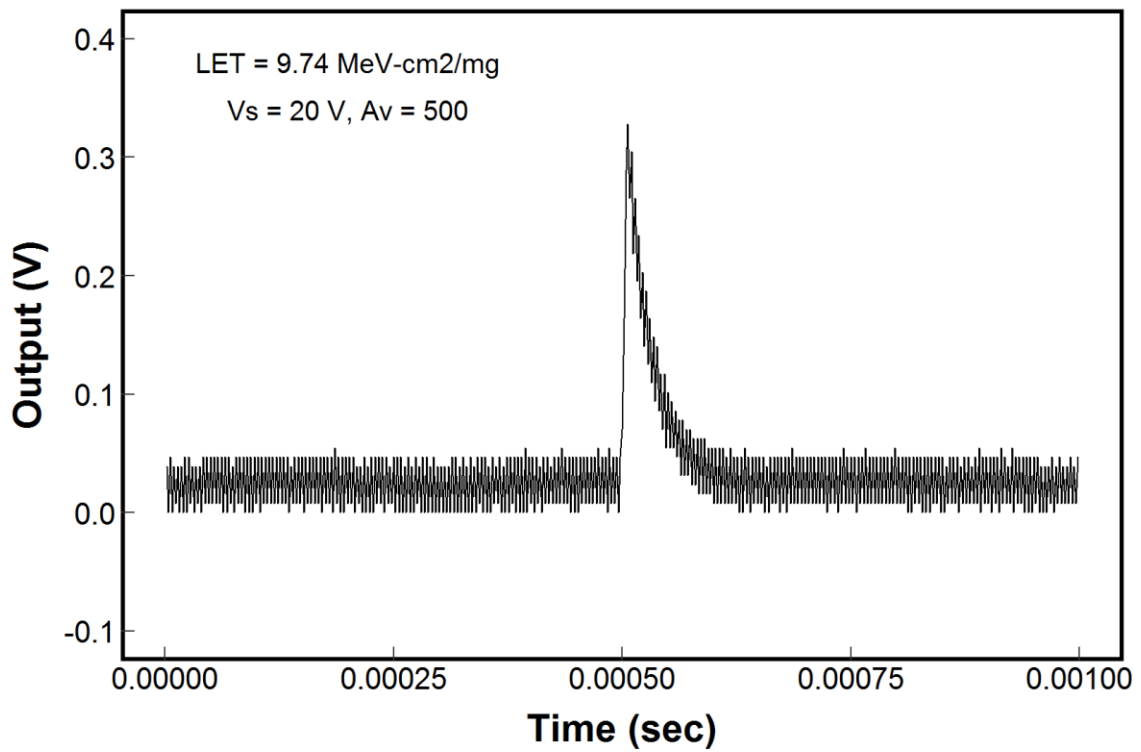


Figure 15. A single-event transient captured at LET of $9.74 \text{ MeV}\cdot\text{cm}^2/\text{mg}$ for $V_s = 30 \text{ V}$ and $A_v = 500$.

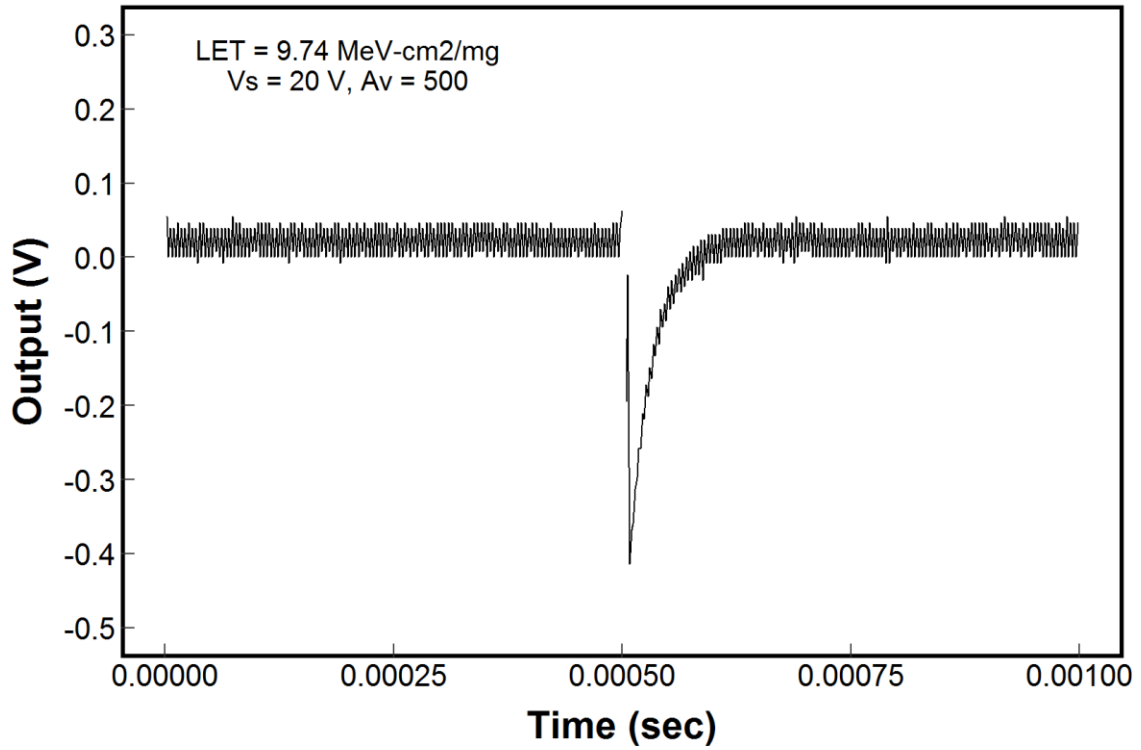


Figure 16. A single-event transient captured at LET of 9.74 MeV·cm²/mg for V_S = 30 V and A_V = 500.

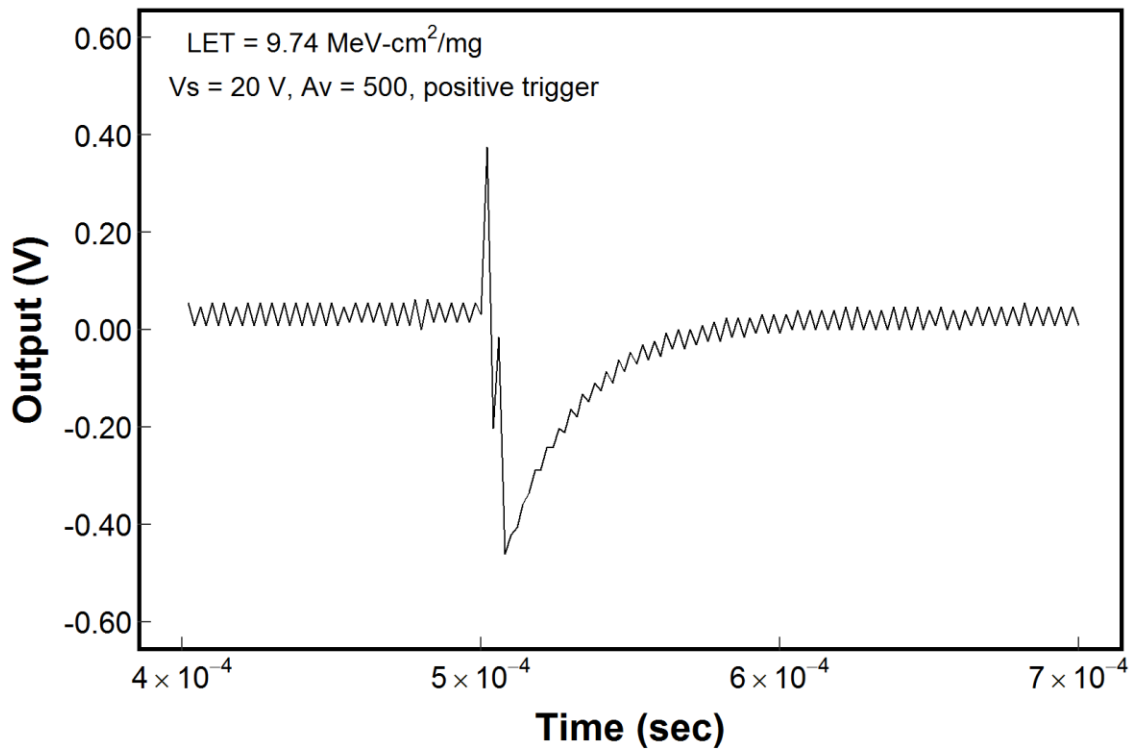


Figure 17. A single-event transient captured at LET of 9.74 MeV·cm²/mg for V_S = 30 V and A_V = 500.

VI. Conclusion

We determined that the RH6105MW is robust against destructive or high current event up to an effective LET of $83.2 \text{ MeV}\cdot\text{cm}^2/\text{mg}$ for the applied test conditions. The device was susceptible to SET. The SETs had durations of 10^3 's of μsec to $\sim 1 \text{ msec}$. Most of the SETs had amplitude less than 2 V, although a small portion of SETs had amplitudes as high as 8 V or higher. We also observed enhanced SET cross section at 60° incident angle relative to irradiations at lower angles with a similar effective LET. In addition, we examined two circuit configurations with different dc gains. The SETs generally had longer duration and larger amplitudes for the higher gain configuration.

VII. Reference

1. Analog Devices, Inc. (2017) "*RH6105 - Radiation Hardened Micropower Precision, Rail-to-Rail Input Current Sense Amplifier*" [Online]. Available: <http://www.analog.com/en/products/rh6105.html#product-overview>, Accessed on: August 27, 2018.
2. Michael B. Johnson, Berkeley Lawrence Berkeley National Laboratory (LBNL), 88-Inch Cyclotron Accelerator, Accelerator Space Effects (BASE) Facility <http://cyclotron.lbl.gov>.
3. JEDEC Government Liaison Committee, Test Procedure for the Management of Single-Event Effects in Semiconductor Devices from Heavy Ion Irradiation, "JESD57, <http://www.jedec.org/standards-documents/docs/jesd-57>, Dec. 1996.